Synthesis of Single-Walled Carbon Nanotubes in Flames

Michael D. Diener,* Noah Nichelson, and John M. Alford

TDA Research, 12345 West 52nd Avenue, Wheat Ridge, Colorado 80033

Received: March 31, 2000; In Final Form: June 26, 2000

The synthesis of single-walled carbon nanotubes (SWNTs) in sooting flames is reported. This method offers a viable path towards low-cost large-scale synthesis, which is lacking in arc- and laser-based SWNT synthetic techniques. As with other methods, the growth of the SWNTs in the flame is catalyzed by the presence of metals. Iron and nickel were introduced into the flames by subliming their bis(cyclopentadienyl) derivatives into an inert gas feed line that mixes with the hydrocarbon fuel and oxygen at the burner surface. Acetylene and ethylene are both suitable fuel choices for SWNT synthesis. While no SWNTs could be detected when benzene was used as the fuel, long metal-filled multiwalled nanotubes (MWNTs) with many defects were abundant. The effect of the fuel's chemical identity is discussed within the formation mechanisms for vapor-grown carbon fibers (VGCFs), SWNTs, MWNTs, and fullerenes.

Introduction

The unique electronic properties and excellent physical characteristics of single-walled carbon nanotubes[1] (SWNTs) have stimulated an intense search for a synthetic process that could be performed cost-effectively at an industrial scale. Originally, SWNTs were synthesized in the condensing graphite/transition metal vapor created by ablation of composite targets by lasers[2] or electric arcs.[3] More recently, they have been produced both by pyrolysis of hydrocarbon/metallocene mixtures flowing through tube furnaces[4] and by catalytic decomposition of CO[5] and hydrocarbon gases over ultrafine supported metal particles at elevated temperatures.[6] We report here the synthesis of SWNTs in fuel-rich acetylene and ethylene surface-mixing flames when metallocenes are added to the flame.

The most pressing issues for SWNT technology are the availability, cost, and purity of the SWNTs. Currently, laser, arc, and chemical vapor deposition (CVD) preparation techniques have the crucial role of supplying researchers with the material necessary for characterization of SWNT properties and predicting SWNT applications. For applications in energy storage or materials reinforcement, however, tons of SWNTs will be required. A report of "large-scale" synthesis of SWNTs from an arc resulted in less than 2 g of SWNTs.[7] The arc process is a labor-intensive batch process and is unlikely to produce more than 1 kg of SWNT soot per day. While its ability to grow the SWNTs where they are required makes the CVD method apparently useful for nanotube electronic device synthesis and integration into more conventional electronic architectures,[8] the supported catalyst imposes severe limitations on the scale and SWNT growth rate. A very recent report of "large-scale synthesis" by CVD produces 1 g of SWNTs per day.[9] None of the above techniques have the potential to supply SWNTs in ton quantities. Nor will they ever has the ability to supply SWNTs at the prices required for fuel cell and composite applications. Purity is also an issue, since, after purification, only ca. 3 wt. % of the original SWNT soot mass remains. This may be due to either the purification technique destroying the SWNTs or SWNT yields being much lower than would appear from the published electron microscope pictures of SWNT soot. We conclude that a new technique for SWNT production is needed, one that builds on the chemistry empirically established by the extensive arc, laser, and CVD laboratory preparation techniques.

The recently publicized HiPCO process[10] is a dramatic improvement in SWNT production. The process can, in principle, be operated continuously, and generates tubes of very high purity. With further development, it should be possible to scale the HiPCO process to large capacities. The success of the HiPCO technique is founded on two of the fundamental truths of SWNT formation: (1) Using CO as the carbon source, while eliminating other sources of carbon (e.g., those associated with the catalyst), will increase purity by eliminating soot-forming side reactions and (2) high pressures are required to drive the catalytic decomposition of CO. However, it is whether that it represents the most immediate or cost-effective route for producing truly large-scale quantities of SWNTs.

The production of SWNTs in sooting flames offers another potentially effective route for synthesis of SWNTs. Sooting flames have an intrinsically cheaper source of process heat than any other technique and are also widely used to produce commercial carbon products. However, the chemistry in a sooting flame is significantly different than that found in arc and laser apparatuses, due to lower maximum temperatures and the presence of hydrogen. This report provides a crucial demonstration of the SWNT formation chemistry in a sooting flame, although the production conditions investigated so far are not nearly optimized. We have also attempted to understand the mechanisms of formation of SWNTs in sooting flames so that the technique can be optimized in a rational manner.

Experimental Section

A schematic of TDA Research's reduced pressure combustion materials synthesis apparatus is shown in Figure 1. It was designed for the synthesis of fullerenes; as such its maximum operating pressure is 80 Torr. Mass flow controllers were used to meter the oxygen and hydrocarbon gas flows. Experiments with benzene were conducted by using a high-performance liquid chromatography pump to convey the liquid benzene to a

*Corresponding author: e-mail mikee@tda.com.

10.1021/jp001233f CCC: $19.00
Published on Web 09/14/2000

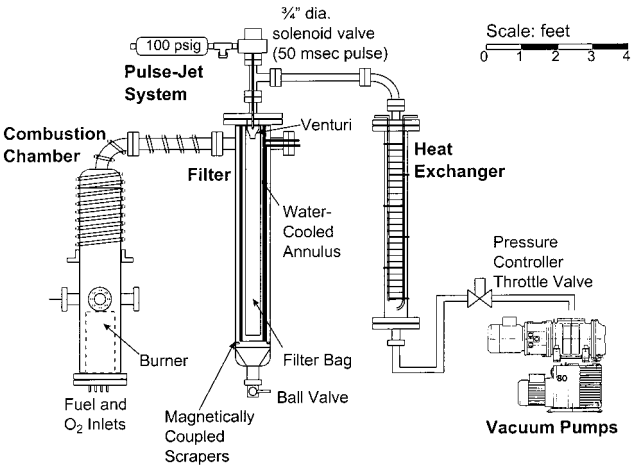

Figure 1. TDA Research's reduced-pressure combustion materials synthesis apparatus, capable of 100 mL/min benzene flow under fullerene-forming conditions.

boiler, and maintaining 150 °C between the boiler and the burner. The fuel and oxidizer feed lines separately pass through the 16-in. diameter flange that forms the bottom of the combustion chamber and continue up into the burner. The fuels were delivered to the burner surface through 155 $^3/_{16}$-in. stainless steel tubes that are evenly spaced within a 4-in. diameter stainless tube. The oxygen flows up through a metal frit welded within the 4-in. tube, and around the $^3/_{16}$-in. tubes. The fuel and oxygen diffuse rapidly into each other at the tips of the $^3/_{16}$-in. tubes under the reduced pressure operating conditions.

Iron, cobalt, and nickel are all known to catalyze the formation of SWNTs from carbon and hydrocarbon vapors. Fe and Ni were introduced into the flame by subliming ferrocene (Aldrich) and nickelocene (Alfa AESAR) powders from a packed bed into an argon stream, which later joins the fuel feed line. The temperature of the bed controls the vapor pressure of the metallocene and thus the addition rate for a given gas flow over the bed. For cobalt, the room-temperature liquid bis-(cyclopentadienyl)cobalt dicarbonyl (Strem) was introduced into the flame by bubbling argon into the liquid reservoir and mixing that vapor stream with the fuel feed line.

Under normal tube-forming conditions, the flame had the yellow-orange color characteristic of soot particle emission. The presence of catalyst was verified by reducing the fuel flow and observing the brightly colored metal emission present during lean conditions. The soot particles, as well as the SWNTs, were carried by the exhaust gas onto a water-cooled annulus and ceramic filter bag. The soot was shaken off the bag periodically by a pulse jet system, and a translatable ring of air jets cleaned the annulus. The soot was then collected out the bottom of the baghouse chamber. Alternately, samples of the soot could be collected from the gas stream between the combustion chamber and the baghouse and removed from the apparatus without discontinuing its operation.

Experiments were conducted with 1.25 standard liters per minute (SLPM) of benzene or 3.75 SLPM of either acetylene or ethylene. The oxygen flow was varied to give equivalence ratios[11] between 1.7 and 3.8. The resulting soot was sonicated into methanol and suspended on a transmission electron microscope (TEM) grid (Structure Probe Inc.) for analysis. Either the Philips 320 TEM with charge-coupled device (CCD) at the National Renewable Energy Laboratory (NREL, Golden, CO) or the Philips 200 TEM at Colorado School of Mines (CSM, Golden, CO) was used for sample analysis.

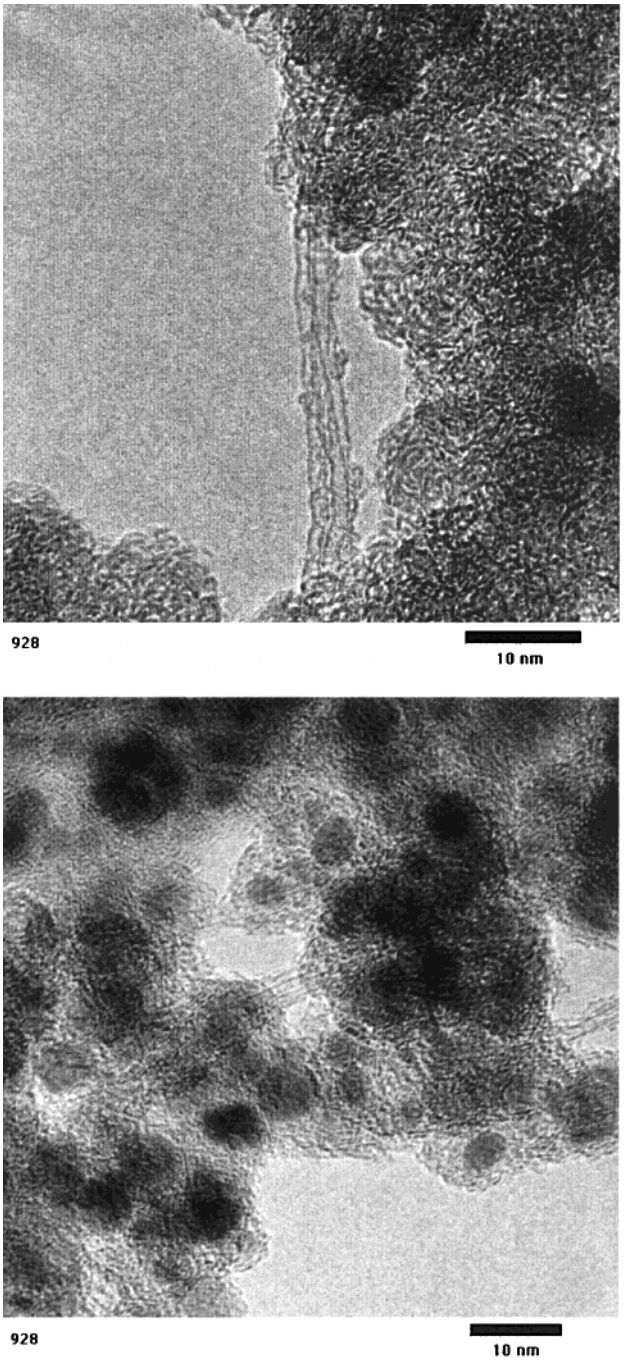

Figure 2. SWNT bundles from sooting acetylene flames in the presence of Fe/Ni catalyst particles. Note the lattice fringes from the metal particle in the lower right of the bottom panel.

Results

Figure 2 displays images from the NREL TEM of the SWNTs in the soot from an 80 Torr acetylene flame with a ferrocene/nickelocene mixture as the catalyst. Tubes in the soot are primarily single-walled, although a thorough search revealed a few MWNTs (we estimate <5% of all tubes). Cobalt addition also resulted in the formation of SWNTs. The metal content of the soot was analyzed after the run by atomic absorption and varied between 0.025% and 2.25 wt %. The overall SWNT yield (certainly less than 1% of the carbon soot product) of the acetylene and ethylene flame soots, regardless of catalyst, is low, by comparison to both high-yield portions of graphite arc SWNT soot and laser-produced SWNTs.

Figure 3. Metal-filled MWNTs from a sooting benzene flame with cobalt introduced as the catalyst.

The type of nanostructured carbon present in the soot varied according to the identity of the feedstocks. Both acetylene and ethylene flames contained SWNTs, with a few MWNTs (again, <5% of all tubes). Although many experiments were conducted with benzene, varying the equivalence ratio between 1.7 and 3.4, the catalyst mixture through single and binary combinations of the three metals, and gas pressure from 30 to 80 Torr, no SWNTs were ever observed. However, MWNTs with many defects, sporadic metal filling, and lengths exceeding 10 μm could be readily observed in the soot from benzene flames operating across a wide variety of conditions (Figure 3). The presence of more catalyst in the benzene flames apparently led to a greater abundance of MWNTs. We estimate that as much as 10% of the solid carbon production could be MWNTs under these conditions. Without any metallocenes present, TEM examination of benzene flame soots revealed mostly soot particles, with a few buckyonions, and a few multiwalled, closed graphitic nuggets with aspect ratios of three or less. Such multiwalled carbon nanostructures with similarly small aspect ratios have previously been observed in premixed flames without catalyst addition.[12]

Discussion

It was surprising to find that SWNTs could not be produced from benzene flames under conditions identical to SWNT-producing acetylene and ethylene flames. The problem is particularly interesting because most (but not all!) of the benzene rings are rapidly broken into acetylenic pieces during combustion.[13] The dependence on hydrocarbon feed is not unique to flames. Pyrolysis experiments provide analogous results: SWNTs have been formed when acetylene and ferrocene (or nickelocene) vapor are mixed in a tube furnace.[4] However, when benzene is substituted for the acetylene, only metal-filled, highly kinked MWNTs are observed.[14] While the temperatures in benzene flames may differ from acetylene flames, the pyrolysis experiments were both conducted at the same temperature (1100 °C). This implies that the SWNT growth dependence on hydrocarbon feedstock is correlated to the chemistry of the hydrocarbon rather than the flame temperature. This section is therefore primarily concerned with understanding the role of hydrocarbon feedstocks in SWNT formation.

The results could be understood if the reaction pathways in competition with SWNT growth dominate for benzene but not for acetylene/ethylene. Soot formation competes with SWNT growth for the carbon in both benzene and acetylene flames. The mechanisms for soot formation have been studied extensively, and it has been found that soot formation proceeds via polyaromatic hydrocarbon (PAH) intermediates. The PAHs begin from a single aromatic ring and can grow by both addition of acetylenic species and condensation of aromatics.[15] The acetylene and ethylene flames must grow the first ring, while it is already present in benzene flames. Thus, PAH and subsequent soot formation begins earlier in benzene flames than in acetylene flames.[16] It is possible that, in benzene flames, soot formation begins at a time where the metal particles have not yet grown large enough to be SWNT catalysts. However, the presence of the metal-filled MWNTs in both benzene flames and benzene pyrolysis demonstrates that some of the benzene (or PAH) is indeed interacting with the metal particles but that the interaction does not lead to SWNT formation. Furthermore, the fact that most of the benzene is broken into acetylenic units prior to PAH formation indicates that acetylene is abundant at times when the metal particles are suitably sized. Therefore, it can be concluded that the competing soot formation pathway is not solely responsible for preventing SWNT formation from benzene. Indeed, the gross similarity of the chemical environments in different flames suggest that benzene goes beyond merely not forming SWNTs but that it poisons the SWNT formation process. Benzene seems to stimulate a different kind of chemistry with the metal particles, which leads to highly defective, metal-filled MWNTs.

The cause of the hydrocarbon dependence must therefore lie in the chemistry of the precursors during the SWNT formation process. The interaction of hydrocarbon and metal leading to filamentous carbon formation has long been widely studied.[17] Until the early 1970s, research had always been aimed at the *prevention* of filamentous carbon growths associated with small metal particles. Historically, filamentous carbon signaled deactivation of catalyst particles or the plugging of a heated steel tube for conveying hydrocarbons in a reactor. The idea that filamentous coke was actually useful (as a high-strength form of carbon fiber), and the subsequent research on its mass production, led to a new moniker for these previously disdained growths, vapor-grown carbon fibers (VGCFs). Even more recently, carbon nanotubes have come to be known as the carbon filaments exclusively made of rolled concentric graphitic sheets. Most VGCFs, however, exhibit a herringbone structure, where graphite-like stacks of carbon planes are canted with respect to the fiber axis.

There are many similarities between SWNT and VGCF growth. The observed temperature range for VGCF formation is consistent with that of SWNTs. SWNTs have never been observed without the presence of transition-metal catalyst particles, and the yield of SWNTs is sensitive to which metal(s) is(are) available. The same metals (Fe, Co, Ni) that have been found to be useful for SWNT synthesis have long been employed for VGCF synthesis. The experimental technique and

apparatus for VGCF growth and many SWNT pyrolysis experiments is essentially the same. As with VGCF cores, MWNTs and SWNTs are commonly coated in pyrolytic carbon resulting from the chemisorption of hydrocarbons on the tube walls. The major dissimilarity is the size of the catalyst particle: for VGCFs, it is usually hundreds of nanometers in diameter, while for SWNT growth, a diameter of a few nanometers is more commonly observed.

The obvious broad similarities in the chemicals and conditions for catalytic growth of SWNTs and VGCFs from hydrocarbons suggest that the model for VGCF formation[17−19] can also be applied to SWNTs, with a few modifications. While the macroscopic similarities between VCGF and MWNT growth have recently been compared,[20] the focus in this work is on the more detailed, chemical mechanism required to understand the effects of the hydrocarbon feed. The model can be briefly summarized in terms of its five steps: (1) absorption of the hydrocarbon gas molecules on the surface of a metal particle, (2) dehydrogenation and dissociation of the hydrocarbon on the metal surface, (3) transport of the carbon from surface to subsurface sites in the particle, (4) diffusion of carbon through the particle, and (5) transfer of carbon from the particle into the filament. While there are still many unresolved issues within this model, it provides a framework for discussion of SWNT formation from hydrocarbons. Examination of the first two steps for both benzene and acetylene will demonstrate how the benzene fails and why small hydrocarbons (or CO) are good choices for SWNT production.

The first step, absorption of the hydrocarbon onto the metal particles, is likely to proceed at about the same rate for benzene as for acetylene. The differences in size and mass indicate that benzene molecules will have about $^2/_3$ as many collisions as acetylene molecules with metal particles of a few nanometers diameter, assuming similar number densities and temperatures. While the chemical environment of flames is far more complex than that of the pyrolysis experiments, and the feedstock must compete for catalyst surface sites with CO, H_2, H_2O, and CO_2, all of these species are present in all of our hydrocarbon flames, in amounts that are dependent more on the equivalence ratio than on the hydrocarbon fuel. Theoretical investigations have shown that the binding energy of benzene to the faces of two- or three-layer Ni cluster is constant for clusters with at least 25 atoms (ca. 0.25 nm diameter),[21] which suggests that the SWNT catalyst particles are probably not small enough to exhibit a size effect for benzene adsorption. Thus, while collision frequencies indicate that acetylene will be mildly favored over benzene, the key to understanding the fuel dependence is unlikely to lie in the absorption step.

The detailed mechanisms of hydrocarbon dissociation on metal surfaces and the disposition of carbon atoms near the surface, as reported in the extensive surface science literature of the past two decades, serve as a guide for understanding the second step in filamentous carbon growth. Dehydrogenation mechanisms have been studied extensively for acetylene, ethylene, and benzene on a variety of single-crystal surfaces. Among active catalysts for SWNT growth from hydrocarbons, the metal whose surfaces are most commonly studied is nickel, which we shall take as representative of SWNT catalysts. Ethylene was observed to dehydrogenate to surface-bonded acetylenic species at low temperatures, and the loss of two hydrogen atoms to C_2H_2 at very low temperature is known on Ni(111).[22] The rate of the reverse reaction, $C_2H_3 + H \rightleftharpoons C_2H_4$ (all species adsorbed), is negligible on Ni[23] when no other source of hydrogen is present. So the similar results for both ethylene and acetylene flames are not surprising in light of the surface science results. Chemisorbed C_2H_n ($n = 2, 3$) on nickel surfaces continues to dehydrogenate and dissociate, forming a surface carbide between 300 and 380 K on both Ni(100)[23,24] and Ni-(111).[25] In comparison, the temperature at which the benzene molecules adsorbed on nickel dehydrogenate is competitive with the temperature for their desorption, and that temperature is 100 K higher than the beginning of chemisorbed acetylene decomposition for similar exposures and surfaces.[26,27] This higher temperature is indicative of a slower dehydrogenation rate for benzene than for either acetylene or ethylene. The temperature difference between acetylene and benzene for their complete molecular dissociation to surface carbide will be further exacerbated by the difference in the number of bonds to be dissociated in the molecules. The slow decomposition of benzene on metal catalyst surfaces is the first part of the reason it is unsuitable for SWNT growth.

The second part is the effect of the catalyst particle size on its ability to completely dissociate the hydrocarbon. There is ample literature to describing classes of metal-catalyzed reactions in terms of the size of the metal particles in the dispersion.[28] It has been determined that hydrogenation and dehydrogenation reactions (addition or loss of H_2 to an adsorbed molecule) are typically insensitive to the size of the metal particle, while rates of hydrogenolysis reactions (where C−C bonds are also broken) are strongly dependent on the particle size. The hydrogenolysis reactions are thought to require a minimum area of homogeneous metal surface (not high-curvature particle edges). According to the VGCF model for filamentous carbon growth, the C−C bonds in the hydrocarbon precursor are broken on the catalyst particle surface. There should therefore be a strong rate effect that is dependent on catalyst particle size. However, this effect is largely masked by the additional, unrelated role of the particle size in producing a certain filament type (i.e., VGCFs on larger particles, SWNTs on smaller particles; step 5). Yet the effect of particle size on decomposition could perhaps be observed by increasing the size of the hydrocarbon to be dissociated and keeping the particle size constant. Such an experiment has already been performed for the larger particles suitable for VGCF growth, and a size effect is indeed observed: VGCFs were grown from benzene, acetylene, and even methylnaphthalene on 70 nm diameter metal particles, but their growth was severely hindered when the larger PAHs fluorene and pyrene were the hydrocarbon feed.[29] We believe it is this same effect, scaled to smaller particles and smaller hydrocarbons, that prevented SWNTs from growing in benzene flames. Catalyst particles that lead to SWNT growth are seemingly too small to dissociate the benzene in the time provided for SWNT growth in our experimental setup.

There are therefore two contributing reasons for smaller hydrocarbons to completely decompose faster than benzene on the metal catalyst particles, but the question of what happens to the benzene carbon atoms remains. As alluded to above, desorption is competitive with dehydrogenation for moderate to high coverages on single-crystal surfaces, suggesting the outcome for some of the benzene molecules. However, after (partial) dehydrogenation has occurred (recall that even small catalyst particles or atoms can perform dehydrogenation), the benzene remnant is stuck on the surface of a particle too small to finish the decomposition. We theorize that the loss of hydrogen in benzene prior to C−C bond scission is likely to serve as a nucleation point for a graphitic overlayer on the catalyst particle. As other adsorbing hydrocarbons collide with the benzene remnant, a PAH could be formed, much as the first

ring is required for PAH growth in acetylene flames. As the (partially hydrogenated) surface-adsorbed PAH becomes larger, it will be a nucleus for the graphite layer, much as planar PAHs grow by acetylene addition in the gas phase. The formation of a graphite layer encircling the catalyst particle will deactivate the catalyst, forming nanoencapsulates rather than filamentous carbon. Every sticking collision between a benzene and the particle surface therefore leads to the deactivation of that particle for SWNT formation, the poisoning effect observed in the experiments. It is also possible that collision between such nanonuggets would form chains when they collide in the gas phase, by analogy to the chains of soot particles commonly observed in flames. Such chains of nanoencapsulates would be expected to have regions of graphitic layers surrounding metals, joined by less-structured areas where the nuggets met and condensed. Such a structure would resemble the metal-filled MWNTs observed here and in pyrolysis.[14] The differences in surface chemistry appear to be the fundamental reasons for the distinctions between benzene and acetylene (or ethylene) flame and pyrolysis techniques for SWNT growth.

Continuing with the VCGF model, the third step predicts that carbon atoms bonded to the Ni surface (forming the surface carbide) are drawn down into subsurface sites. Darling, Pendry, and Joyner[30] have reported on the electronic origins of this force and further comment that there is no force to push the carbidic carbon atoms away from the surface (into a graphitic overlayer). For single-crystal nickel at sufficiently high temperatures (vide infra) and sufficiently large particles, the surface carbon is drawn down into subsurface sites. This holds true regardless of whether the carbidic surface carbon came from the decomposition of C_2H_n or benzene.[31]

The diffusion of subsurface carbon atoms into the particle bulk is the fourth step of the VGCF growth model. A quick calculation[32] of the diffusion coefficient for interstitial carbon atoms in a nickel lattice shows the importance of high temperature for filamentous carbon growth and explains graphitic layer formation from carbides (via an intermediate state) in clean single-crystal surface studies.[33] Bulk metal carbides of Fe, Co, and Ni have the carbon atoms placed at sites interstitial in the lattice of the pure metal. The diffusion coefficient for interstitial hopping from just below the surface into a carbon-free lattice is given by $D = a\upsilon/3 = (a^2\omega/3\pi)\exp^{-E/kT}$, where a is the distance between the interstitial sites, υ is the speed of the carbon atoms, ω is the oscillator frequency for a carbon atom from the Debye approximation, E is the magnitude of the potential energy barrier between two interstitial sites (which is also the activation energy for carbon diffusion), k is Boltzmann's constant, and T is temperature. E has been measured for nickel at 145 kJ/mol,[34] for cobalt at 139 kJ/mol, and for γ-Fe at 142 kJ/mol.[18] The lattice constant for nickel is 0.352 nm. Atomic oscillator frequencies are on the order of 10^{14} s^{-1}, with about an order of magnitude of uncertainty. Combining these data shows that there is essentially no movement of the carbon on a 1 ms time scale at temperatures up to 600 K. The carbon sites immediately below the surface are therefore rapidly filled, and the carbidic carbon transforms into the graphitic overlayer observed in the surface science literature in this moderate temperature range.[33] Conversely, at 1300 K, an average temperature for SWNT formation, less than 1 ms is required for the carbon to race through a 10 nm particle. Therefore, the higher temperatures, by promoting diffusion, free the subsurface sites and allow transfer of carbon from the carbidic layer into the particle rather than into a graphitic layer. This is in concert with surface science results where the surface is heated rapidly to high temperature[31] and also with the acceptable temperature range for filamentous carbon growth. The temperatures that qualify as "moderate" for graphitic layer growth and "higher" for transfer to subsurface sites depend on the carbon concentration.[35]

Although it has long been assumed that the diffusion of carbon through the particle is the rate-limiting step for the formation of VGCFs,[18] the different results from different hydrocarbon precursors demonstrates that that is not always the case. The difficulties of growing VGCFs from pyrene and fluoranthrene[29] and SWNTs from benzene clearly show that the decomposition processes occurring on the particle surface can be rate-limiting. That diffusion through the particle should be the rate-limiting step has been previously questioned[19,36] when CO is the precursor.

Finally, we contrast some aspects of fullerene and SWNT formation. The dependence of the hydrocarbon fuel's chemical identity for SWNT synthesis is directly opposed to that for the combustion synthesis of fullerenes. The formation of fullerenes in flames is thought to proceed from a phenyl ring through polycyclic aromatic hydrocarbons (PAHs), which knit together ("aromers")[37] and/or grow by acetylene addition[38] and (in the correct pressure and temperature range) finally rearrange to become a fullerene.[39] Acetylene flames are barely capable of producing fullerenes, while indene flames have even higher fullerene yields than benzene flames.[40] This is because the growth from acetylene into a phenyl ring occurs relatively slowly in comparison to ring growth reactions, while uncombusted benzene seeds PAH formation, jump-starting fullerene formation. The best fuels for combustion synthesis of fullerenes are therefore the worst for combustion synthesis of SWNTs, and vice-versa. It may be possible to produce SWNTs in an acetylene flame without a lot of soot byproduct, if all of the acetylenic carbon can be converted to SWNTs before soot formation is initiated.

Further contrast is provided by the difference in optimum pressures for fullerene and SWNT growth. Fullerene formation is a relatively delicate process; 30 Torr is typically the optimum condition for fullerene growth in our flames. Higher pressures increase the gas-phase collision rates between partially dehydrogenated PAHs and other hydrocarbons, leading toward the kinetically favored soot particles and large PAHs rather than the thermodynamic fullerene product (also see ref 39). For SWNT growth by combustion or pyrolysis, following a sticking collision with the catalyst particle surface, the hydrocarbon can either desorb or dehydrogenate. Since desorption is inversely related to pressure, higher pressures are generally favorable for SWNT growth according to the model presented above (although it seems possible that much pressure could increase the collision rate to a point where carbon is added to the surface faster than it can migrate to available subsurface sites, with the result of deactivating the catalyst particle.) Pyrolysis[4] and CVD[5,6] for SWNT formation is typically performed at near-ambient pressures, adding to our conviction that the pressure range available to our fullerene apparatus is too low for the optimum synthesis of SWNTs by combustion. We are currently constructing an apparatus capable of operation at ambient pressure with small hydrocarbon flames, in the hope of dramatically increasing our SWNT yield.

Summary

We have demonstrated the formation of SWNTs from small hydrocarbon precursors in fuel-rich flames and commented extensively on the mechanism for catalytic SWNT formation.

As hydrocarbon feedstocks, acetylene and ethylene are strongly favored over benzene because of the slower dissociation rate of benzene on nanometer-sized metal particles. For SWNTs, both fuel and pressure dependence are opposite to those observed for fullerene formation. The flame synthesis technique offers several advantages for the industrial-scale production of SWNTs over the current arc, laser, and batch pyrolysis apparatuses, including cheaper heat and continuous processing. Improved mixing of reagents in the gas phase should also lead toward increased yield, but that will only be apparent when the flame is operated in the correct pressure range.

Acknowledgment. We thank K. M. Jones at the National Renewable Energy Laboratory (Golden, CO) for HR-TEM analysis (Figure 2) and B. McGrew at Colorado School of Mines for additional TEM analysis (Figure 3). We also acknowledge S. Gebhard and J. W. Wright at TDA, T. McKinnon at Colorado School of Mines, and D. Ramaker at the Naval Research Laboratory (Washington, DC) for insightful discussions. This work was funded by a NASA Phase I SBIR grant, NAS-9-98066.

Note Added in Proof. The synthesis of SWNTs in atmospheric pressure laminar diffusion flames has recently been reported.[41]

References and Notes

(1) Recent reviews: (a) Ajayan, P. *Chem. Rev.* **1999**, *99*, 1787. (b) Ebbesen, T., Ed. *Carbon Nanotubes: Preparation and Properties*, CRC Press: Boca Raton, FL, 1997. (c) Saito, R.; Dresselhaus, M.; Dresselhaus, G. *Physical Properties of Carbon Nanotubes*; Imperial College Press: London, 1998.

(2) Guo, T.; Nikolaev, P.; Thess, A.; Colbert, D. T.; Smalley, R. E. *Chem. Phys. Lett.* **1995**, *243*, 49.

(3) (a) Iijima, S.; Ichihashi, T. *Nature* **1993**, *363*, 603. (b) Bethune, D. S.; et al. *Nature* **1993**, *363*, 605.

(4) Satishkumar, B.; Govindaraj, A.; Sen, R.; Rao, C. N. R. *Chem. Phys. Lett.* **1998**, *293*, 47.

(5) Dai, H.; et al. *Chem. Phys. Lett.* **1996**, *260*, 471.

(6) (a) Hafner, J.; et al. *Chem. Phys. Lett.* **1998**, *296*, 195. (b) Kong, J.; Cassell, A.; Dai, H. *Chem. Phys. Lett.* **1998**, *292*, 567.

(7) Journet, C.; et al. *Nature* **1997**, *388*, 756.

(8) Dai, H.; et al. *J. Phys. Chem. B* **2000**, (in press).

(9) Colomer, J.; et al. *Chem. Phys. Lett.* **2000**, *317*, 83.

(10) Dagani, R. *Chem. Eng. News* **2000**, *78*, 36.

(11) The equivalence ratio, Φ, is defined as "the actual fuel/oxidzer ratio divided by the stoichiometric fuel/oxidizer ratio" in Glassman, I. *Combustion*; Academic Press: Orlando, FL, 1987; p 20.

(12) (a) Howard, J.; Das Chowdhury, K.; VanderSande, J. *Nature* **1994**, *370*, 603. B) Das Chowdhury, K.; Howard, J.; VanderSande, J. *J. Mater. Res.* **1996**, *11*, 341.

(13) Bittner, J.; Howard, J. *Eighteenth Symposium (International) on Combustion*; The Combustion Institute: Pittsburgh, PA, 1981; p 1105.

(14) Sen, R.; Govindaraj, A.; Rao, C. *Chem. Phys. Lett.* **1997**, *267*, 276.

(15) McKinnon, J.; Howard, J. *Twenty-Fourth Symposium (International) on Combustion*, The Combustion Institute: Pittsburgh, PA, 1992; p 965.

(16) For further review of soot formation in flames, the reader is referred to *Soot Formation in Combustion*; Bachman, R., Ed.; Springer-Verlag: Berlin, 1994.

(17) Rodriguez, N. M. *J. Mater. Res.* **1993**, *8*, 3233.

(18) Baker, R. T.; Barber, M. A.; et al. *J. Catal.* **1972**, *26*, 51.

(19) Alstrup, I. *J. Catal.* **1988**, *109*, 241.

(20) Sinnott, S.; et al. *Chem. Phys. Lett.* **1999**, *315*, 25.

(21) Grimm, F. A.; Huntley, D. R. *J. Phys. Chem.* **1993**, *97*, 3800.

(22) Demuth, J. E.; Eastman, D. E. *Phys. Rev. Lett.* **1974**, *32*, 1174.

(23) Zaera, F.; Hall, R. *Surf. Sci.* **1987**, *180*, 1.

(24) Hutson, K. F.; Ramaker, D. E.; Koel, B. E.; Gebhard, S. C. *Surf. Sci.* **1991**, *248*, 119.

(25) Hammer, L.; Dotsch, B.; Harder, C.; Muller, K. *Vacuum* **1990**, *41*, 121.

(26) Steinruck, H. P.; Huber, W.; Pache, T.; Menzel, D. *Surf. Sci.* **1989**, *218*, 293.

(27) Blass, P.; Akhter, S.; White, J. *Surf. Sci.* **1987**, *191*, 406.

(28) Reviewed by Sinfelt, J. H. Three Decades of Catalysis by Metals; In *Chemistry and Physics of Solid Surfaces VI*; Vanselow, R., Howe, R., Eds.; Springer-Verlag: Berlin, 1986.

(29) Kato, T.; et al. *Carbon* **1993**, *31*, 937.

(30) Darling, G.; Pendry, J.; Joyner, R. *Surf. Sci.* **1989**, *221*, 69.

(31) Huntley, D. R.; Jordan, S. L.; Grimm, F. A. *J. Phys. Chem.* **1992**, *96*, 1409.

(32) A thorough treatment is given by Holstein, W. L. *J. Catal.* **1995**, *152*, 42.

(33) Hutson, K F.; Ramaker, D., Koel, B. *Surf. Sci.* **1991**, *248*, 104.

(34) Baker, R. T. K.; Harris, P. S.; Thomas, R. B.; Waite, R. J. *J. Catal.* **1973**, *30*, 86.

(35) Eizenberg, M.; Blakely, J. M. *Surf. Sci.* **1979**, 228.

(36) (a) Alstrup, I.; Tavares, M. T. *J. Catal.* **1993**, *139*, 513. (b) Nolan, P. E.; Lynch, D. C.; Cutler, A. H. *J. Phys. Chem.* **1998**, *102*, 4165.

(37) Bachmann, M.; Wiese, W.; Homann, K.-H. *Twenty-sixth Symposium (International) on Combustion*; The Combustion Institute: The Pittsburgh, PA, 1996; p 2259.

(38) Pope, C. J.; Marr, J. A.; Howard, J. B. *J. Phys. Chem.* **1993**, *97*, 11001.

(39) Fullerene and PAH formation in flames was recently reviewed: Homann, K.-H. *Angew. Chem., Int. Ed. Engl.* **1998**, *37*, 2434−2451.

(40) As merely measuring the percent extractable fullerenes in the soot neglects the distribution of carbon atoms between the soot and gaseous byproducts, it is crucial to account for the amount of soot produced as well. We therefore define yield as the total number of carbon atoms in all of the xylene-extractable fullerenes produced during the entire run divided by carbon atoms in the fuel consumed during the entire run. All of the soot is collected (where it is incidentally mixed quite thoroughly) and weighed (typically tens to hundreds of grams). A sample (typically tens of milligrams) is removed and sonicated into enough xylene to dissolve the entire sample, were it all fullerenes. High-performance liquid chromatography (HPLC) is then performed on a Waters Spherisorb C18 column with toluene/methanol 60:40 as the mobile phase and the eluent monitored at 308 nm. Peak areas were integrated and compared to our own set of standards for C_{60}, C_{70}, $C_{76} + C_{78}$, and $C_{82} + C_{84}$. Following this procedure and using our apparatus in comparable setups for all fuels, we find the benzene flame yield is 0.38% and the indene flame yield is 0.74%. Under our current best conditions, the percent extractable fullerenes is similar in both flames (∼10%), but the indene flame produces twice as much soot at the same feed rate and equivalence ratio. Also, the purity of the indene fuel feedstock was quite low, with both lighter and heavier aromatics present. We were less thorough in determining the precise optimum conditions for acetylene flames (the mesh size for experimental parameters was larger), but the yield is about 2 orders of magnitude lower.

(41) Vander Wal, R. L.; Ticich, T. M.; Curtis, V. E. *Chem. Phys. Lett.* **2000**, *323*, 217.